URANIUM ISOTOPIC FRACTIONATION INDUCED BY U(VI) ADSORPTION ONTO COMMON AQUIFER MINERALS

BY

NOAH EDWARD JEMISON

THESIS

Submitted in partial fulfillment of the requirements
for the degree of Master of Science in Geology
in the Graduate College of the
University of Illinois at Urbana-Champaign 2015

Urbana, Illinois

Adviser:

Professor Thomas M. Johnson

ABSTRACT

Uranium groundwater contamination due to mining and processing affects numerous sites in the western United States. Bioreduction of soluble, mobile U(VI) to U(IV)-bearing solids is a common remediation strategy. Uranium isotopes ($^{238}U/^{235}U$) have been utilized to track the progress of microbial reduction, with laboratory and field studies finding a ~1‰ isotopic fractionation with the U(IV) product enriched in ^{238}U. However, the isotopic fractionation produced by adsorption may complicate the use of $^{238}U/^{235}U$ to trace microbial reduction. A previous study found that adsorption of U(VI) onto Mn oxides produced a -0.2‰ fractionation with the adsorbed U(VI) depleted in ^{238}U (Brennecka et. al. 2011b).

The aqueous speciation of U(VI), and the characteristics of the sorbent surfaces may both produce variations in isotopic fractionation induced by adsorption. This study determined U isotopic fractionation induced by U(VI) adsorption onto goethite, birnessite, illite, quartz, and complex aquifer materials. The influence of U(VI) speciation on fractionation was also examined by measuring differences between fractionation factors accompanying the adsorption of uranyl, uranyl hydroxyl, uranyl carbonato, and calcium uranyl carbonato ions. To increase our ability to resolve fractionation, experiments were carried out with a multi-stage, batch approach, in which a U(VI)-bearing solution was exposed to three stages of adsorption. The dissolved U(VI) was analyzed by a double-spike MC-ICP-MS method. Adsorption to the studied solid phases induces an average isotopic fractionation of -0.17‰ with the adsorbed U(VI) isotopically lighter. U(VI) speciation can affect the magnitude of isotopic fractionation with uranyl carbonato and calcium uranyl carbonato complexes producing a greater isotopic fractionation than uranyl hydroxyl species. Studies using U isotope data to assess U(VI) reduction must consider adsorption as a lesser, but significant isotope-fractionating process.

ACKNOWLEDGMENTS

This research could not have been completed without the help of my colleagues, friends, and family. I first want to thank my advisor Dr. Tom Johnson who took my jumbled thoughts and writing and helped turn it into a thesis. I also want to thank Dr. Alyssa Shiel who helped me come up with the idea of researching the isotopic fractionation of U induced by adsorption. Thanks to Dr. Craig Lundstrom who supported me in the lab and kept things interesting. I am very grateful to my fellow graduate students (Gideon Bartov, Nick Huggett, Matt Bizjak, Naomi Wasserman, Joel McKinney, Erin Murphy, Nick Martin, Andy Nash, and Mike DeLucia) who dealt with my odd behavior. Last, but definitely not least, I would like to thank my family, Dave, Doreen, Grace, and Lucas Jemison for keeping me around. Without you all, this would not have been possible.

TABLE OF CONTENTS

CHAPTER 1- INTRODUCTION

Uranium (U) groundwater contamination presents a significant public health hazard, with U mining and milling for nuclear power and weapons generating 938 million cubic meters of mill tailings worldwide over the past several decades (Abdelouas 2006). The frequency of U contamination has led to research on improving the effectiveness and cost efficiency of remediation techniques (Wall and Krumholz 2006; Anderson et. al. 2003; Fox et. al. 2012). The US Department of Energy has supported experiments examining remediation techniques at several U contaminated sites across the country, including sites in Colorado, Arizona, Utah, and Oregon (UMTRCA 2013). To determine the lasting effectiveness of remediation techniques, methods for studying key geochemical processes affecting the fate and transport of U are needed.

The environmental geochemistry of U has been studied in detail and has been summarized in several review articles (e.g., Abdelouas 2006; Wall and Krumholz 2006). U occurs primarily in two oxidation states in aqueous systems: U(VI) and U(IV). U(VI) is soluble and mobile, while U(IV) is relatively insoluble and immobile. When U is reduced from U(VI) to U(IV), the U(IV) precipitates in most groundwater systems, usually as stable U(IV)-bearing solid phases. One groundwater remediation strategy involves the injection of an electron donor, such as acetate, to induce microbial reduction of U(VI) (Anderson et. al. 2003; Wall and Krumholz 2006; Long et. al. 2015). At a U.S. Dept. of Energy site in Rifle, Colorado, USA, experiments have been conducted as part of the Rifle Integrated Field Research Challenge (IFRC), to study the feasibility and systematics of stimulated microbial U(VI) reduction (Anderson et. al. 2003). U-contaminated aquifers may also contain naturally reducing zones with high concentrations of organic carbon and/or reduced metal phases, which can naturally attenuate U(VI) concentrations through reduction (Campbell et. al. 2012).

Redox reactions have exerted a major control over the geochemical behavior of U through time. Sediment hosted U ore deposits were generated by ancient U(VI) reduction, as groundwater containing U(VI) encountered reducing condition in aquifers and produced accumulations of U(IV) minerals (Hobday and Galloway 1999). Over the Earth's history, the global geochemical cycle of U has varied in response to major redox changes. When atmospheric and oceanic redox conditions shifted considerably (e.g. the Great Oxidation Event), the global U cycle changed dramatically, producing sedimentary deposits with differing concentrations of U (Tribovillard et. al. 2006).

In addition to reduction, adsorption of U(VI) to minerals like iron oxides, clays, and quartz is an important geochemical process controlling U mobility and concentrations in natural waters. Adsorption is particularly significant in aquifers, where solid surfaces are abundant. U(VI) can produce both outer- and inner- sphere complexes during adsorption to minerals (e.g., Sylwester et. al. 2000). During outer sphere adsorption, U(VI) ions are attracted to mineral surfaces but are still surrounded by water molecules. With inner sphere complexation, U(VI) directly bonds with the mineral surface (e.g., Sylwester et. al. 2000). Adsorbed U(VI) can desorb in response to changes in pH, bicarbonate concentrations, calcium concentrations, and other groundwater variables. Variations in concentrations of other ions affect U(VI) speciation in natural waters, typically shifting from primarily the uranyl ion (UO_2^{2+}) at low pH (e.g., 3.0) to uranyl carbonato species (such as $UO_2(CO_3)_2^{2-}$ and $UO_2(CO_3)_3^{4-}$) at neutral to high pH and calcium-uranyl carbonato species ($Ca_2UO_2(CO_3)_3^{0}$ and $CaUO_2(CO_3)_3^{2-}$) in the presence of typical groundwater Ca concentrations (Hsi and Langmuir 1985; Fox et. al. 2006). Uranyl carbonato aqueous species, especially those also incorporating calcium, adsorb less to quartz, clays, and iron oxides than the uranyl ion due to the increased stability of the aqueous complexes

relative to uncomplexed uranyl ions (Hsi and Langmuir 1985; Fox et. al. 2006; Stewart et. al. 2010). Therefore when pH, bicarbonate concentrations, and calcium concentrations increase, U(VI) desorbs from minerals and groundwater U(VI) concentrations increase. Increasing bicarbonate concentrations also increase the concentration of carbonate ions, which competitively adsorb to mineral surface sites and hinder the adsorption of U(VI) ions.

Detecting and quantifying U(VI) reduction is often done by determining decreases in dissolved U(VI) concentrations. However, adsorption can also result in decreased U(VI) concentrations. While adsorption can lead to decreased U(VI) concentrations temporarily, desorption can occur rapidly with groundwater chemistry changes like shifts in pH or bicarbonate concentrations (Fox et. al. 2006). The reduction of U(VI) can more effectively, and possibly more permanently, immobilize U(VI) from the groundwater (e.g., Wall and Krumholz 2006). Therefore, another method in conjunction with concentration data is needed to distinguish decreases in U(VI) concentration due to adsorption from those due to reduction.

U isotopes have been developed as a tool to investigate U redox reactions. Chemical reactions can produce shifts in the relative amounts of the two isotopes utilized, ^{238}U and ^{235}U. The isotopic difference in $^{238}U/^{235}U$ between the reactant and product of a reaction (e.g., U(VI) and U(IV) for U reduction) is expressed as a fractionation factor, α:

$$\alpha = {}^{238}U /{}^{235}U_{product} / {}^{238}U /{}^{235}U_{reactant} \qquad (1)$$

The kinetic isotopic fractionation, or shift in the isotopic ratio produced by a kinetic reaction (e.g., U reduction), is more conveniently expressed as a per mil deviation of α from unity, ε:

$$\varepsilon = 1000‰*(\alpha-1) \quad (2)$$

The isotopic fractionation produced by U(VI) reduction by isolated microbes in a laboratory setting varied between 0.6‰ and 1.0‰ with the more rapid reduction of ^{238}U (Basu et. al. 2014; Stylo et. al. 2015). In contrast to microbial reduction, abiotic reduction of U(VI) produced by sulfide, mackinawite (FeS), reduced organic species, and zero-valent zinc appears to result in little to no isotopic fractionation (Stirling et. al. 2007; Stylo et. al. 2015; Grimm et. al. 2014). Field-based measurements indicated that an isotopic shift was produced during the bioremediation of U(VI) at the Rifle IFRC site as injected acetate stimulated microbial reduction. As the microbes reduced U(VI), a shift in $^{238}U/^{235}U$ of approximately -1‰ was observed for the groundwater as the more rapid reduction of ^{238}U led to a greater proportion of ^{235}U in the groundwater (Bopp et. al. 2010). Evidence for enrichment of ^{238}U in U(IV) solids comes from anoxic black shales that average ~0.6‰ heavier (i.e., greater in $^{238}U/^{235}U$) than U(VI) in seawater (Weyer et. al. 2008) and U roll front deposits which are heavier than presumed bulk-earth U by 0.4‰ (Bopp et. al. 2009; Brennecka et. al. 2010; Murphy et. al. 2014). U isotopes have been utilized as a redox tracer of the ancient oceans, investigating redox conditions dating back to the Archean Eon (Montoya-Pino et. al. 2010; Kendall et. al. 2013; Kendall et. al. 2015; Brennecka et. al. 2011a; Dahl et. al. 2014; Asael et. al. 2013). During major redox shifts in the atmosphere and oceans, changes in the redox cycling of U produce U isotope shifts that are preserved in oceanic carbonates and shales.

The isotopic fractionation produced by U reduction is primarily a kinetic isotope effect in nature at most surface temperatures, because isotopic equilibrium between U(VI) and U(IV) can take years to attain (Wang et. al. 2015). Laboratory and theoretical investigations find that if

isotopic equilibrium is attained, U(IV) is about 1‰ heavier than U(VI) (Abe et. al. 2008; Fujii et. al. 2006; Wang et. al. 2015). The enrichment of ^{238}U in U(IV) is believed to result from the nuclear volume effect, which concentrates the heavier isotopes in U species having less electron density near the nucleus. It happens that U(IV) has lesser density, due to shielding by additional f electrons, relative to U(VI) (Schauble 2006; Bigeleisen 1996).

Previous work investigated U isotopic fractionation induced by inner sphere adsorption. In this case, isotopic fractionation is an equilibrium phenomenon in most settings; equilibrium between aqueous and adsorbed U(VI) can be attained in a matter of minutes to hours, much faster than the equilibrium between U(VI)-U(IV) (Brennecka et. al. 2011b; Wang et. al. 2015). Brennecka et. al. (2011b) measured fractionation experimentally by adsorbing aqueous uranyl hydroxyl ions to birnessite ($K_{0.5}Mn^{3+}Mn^{4+}O_4 \cdot 1.5H_2O$) (Wasylenki et. al. 2008). Brennecka et. al. (2011b) found an equilibrium isotopic fractionation of -0.22‰±0.09‰ between the isotopically light adsorbed U(VI) and isotopically heavy aqueous U(VI). This result agrees well with the results of Weyer et. al. (2008) and Goto et. al. (2014), who found a consistent isotopic offset between U(VI) in seawater and ferromanganese crusts. Weyer et. al. (2008) found that the ferromanganese crusts, which are thought to incorporate U(VI) via adsorption, were isotopically light compared to the seawater by an average of 0.17‰. Goto et. al. (2014) found an average isotopic fractionation of -0.24‰ between ferromanganese oxides and seawater, within the uncertainty of the Weyer et. al. (2008) findings.

A field study measured groundwater $^{238}U/^{235}U$ shifts that occurred in response to adsorption and desorption of U(VI) at the Rifle IFRC site. Injected bicarbonate caused desorption of U(VI) from aquifer materials, resulting in dissolved U(VI) concentrations increasing approximately two fold. Following the stoppage of bicarbonate, U(VI) concentrations

decreased to half the initial concentration as U(VI) speciation returned to normal and U(VI) repopulated mineral surface sites (Shiel et. al. 2013). However, through this adsorption-desorption cycle, the U isotopes remained constant within analytical uncertainty (Shiel et. al. 2013). This apparent lack of isotopic fractionation was attributed to differences from the Brenneka et al. (2011b) study, in the sorbents or the dominant U(VI) aqueous species present.

Better understanding of the factors that influence isotopic fractionation related to adsorption of U(VI) would improve methods of monitoring of remediation progress as well as studies using $^{238}U/^{235}U$ to reveal other environmental or geochemical processes. One factor that may affect isotopic fractionation during adsorption is the U(VI) aqueous speciation. The speciation of Brennecka et. al. (2011b) was uranyl hydroxyl ions, a U(VI) species that is not often seen in nature. The ocean and typical groundwaters contain primarily calcium-uranyl carbonato complexes (Klinkhammer and Palmer 1991; Fox et. al. 2006). Additionally, the difference in isotopic fractionation between U(VI) adsorption to birnessite versus adsorption to iron oxides, clay, or quartz is unknown. Using EXAFS (Extended X-Ray Absorption Fine Structure), Brennecka et. al. (2011b) found that the isotopic fractionation induced by U(VI) adsorption to birnessite reflected coordination differences between aqueous U(VI) and adsorbed U(VI). Previous U(VI) adsorption studies using EXAFS found similar coordination changes with adsorption to quartz, clays, and iron oxides (Waite et. al. 1994; Bargar et. al. 2000; Catalano and Brown 2005; Ilton et. al. 2012; Singh et. al. 2012).

Through our research, we aim to predict the isotopic fractionation induced by adsorption in a wide range of geochemical settings. We present results of experiments measuring isotopic fractionation induced by U(VI) adsorption to birnessite, goethite (FeOOH), illite ($K_{0.65}Al_{2.0}[Al_{0.65}Si_{3.35}O_{10}](OH)_2$) (Rieder et. al. 1998), quartz, and complex aquifer materials. In

addition, we explore the influence of U(VI) speciation on the magnitude of fractionation by comparing the fractionation produced by adsorption of uranyl, uranyl hydroxyl, uranyl carbonato, and calcium uranyl carbonato ions. Our study provides the first direct measurement of the isotopic fractionation induced by adsorption of U(VI) species relevant to seawater. The insights gained should improve interpretation of U isotope measurements made in a variety of environmental and geochemical studies.

CHAPTER 2- METHODS

Batch experiments with U(VI)

Table 1 lists the solution and sorbent parameters used in the eight experiments. 125 mL glass serum bottles were used for all U(VI) adsorption experiments. High-purity (18MΩ-cm) deionized water and a solution of 8 ppm U(VI) and 1.25 mM HNO_3 were initially added to a 125 mL vessel to achieve a solution volume of 80 mL and a U(VI) concentration of 1000 ppb. For most experiments, sodium bicarbonate was added to produce uranyl carbonato complexes (Table 1). All experiments with bicarbonate were conducted at pH 8 in order to approximate ocean conditions. We measured pH at the start of experiments and after sampling. The initial pH of bicarbonate experiments was achieved via addition of a small amount of 2% nitric acid; resulting NO_3^- concentrations were <1.1 mM. To produce calcium uranyl carbonato complexes in experiment 6, calcium nitrate was added and contributed an additional 1.8 mM NO_3^-. In experiment 2, a pH of 6 was attained via addition of 25 μM NaOH to an initially acidic solution. The lack of bicarbonate retarded the formation of uranyl carbonato complexes, leaving uranyl hydroxyl ions dominant. Uranyl hydroxyl ions are uncommon in natural conditions, but can provide greater understanding of the influence of U(VI) speciation on isotopic fractionation. Experiment 8 was conducted at pH 3 to form primarily uranyl ions, which are dominant only at low pH. To attain this pH, nitric acid was added, with the final NO_3^- concentration approximately 0.9 mM. All solutions were exposed to air to ensure aerobic conditions and prevent complications from U(VI) reduction.

Substrates chosen for this study were Bayferrox Yellow 910 synthetic goethite, ground Fisher Scientific quartz, illite from Gavi Island off the coast of Italy (Ylagan et. al. 2000), birnessite, and aquifer sediments from the Rifle IFRC site. The birnessite was produced by reducing potassium permanganate with hydrochloric acid (Stroes-Gascoyne et. al.1987). After

precipitation, the birnessite was centrifuged, the supernatant was removed, and the birnessite was washed with DI water. This process was repeated several times to minimize the addition of potassium, permanganate, and chloride ions to birnessite experiments. The aquifer sediments were dried and sieved with particles <250μm utilized for the sediment experiment. Aquifer sediments consisted of quartz, plagioclase, K-feldspar, calcite, clays, and iron oxides (Shiel et. al. 2013). All experiments were well-mixed by placing them on a shaker table.

Multi-step, batch experiments were conducted to equilibrate dissolved and adsorbed U(VI), and precisely determine the magnitude of isotopic fractionation between them. In order to produce significant $^{238}U/^{235}U$ shifts without decreasing the aqueous U(VI) concentration below workable levels for precise isotopic measurements, experiments aimed for 50% adsorption of dissolved U(VI) for each addition of substrate. For each substrate, a preliminary experiment was conducted to determine the concentration of substrate that produced the desired amount of adsorption (Table 1).

Prior to addition of solid sorbent, the U(VI) was equilibrated with the solution matrix by mixing on a shaker table for 24 hours. The sorbent of choice was added as a suspension in DI water. For each of the 8 experiments, a control experiment was conducted with the same U(VI) solution matrix, but without substrates, to monitor U(VI) concentrations without adsorption. After addition of sorbent, the U(VI) solution was allowed to equilibrate for another 24 hour period before the substrate was removed via filtration using 0.22 um filters. We determined that an equilibration time of 24 hours provided an adequate period for aqueous and adsorbed U(VI) to reach isotopic equilibrium after collecting samples at 30 minutes, 2 hours, 24 hours, and 65 hours for uranyl carbonato complexes adsorbing to goethite (see results). After filtration, the U(VI) solution was placed back into a washed glass serum bottle. A second round of substrate was then

added to the U(VI) solution. The substrate was again removed via filtration after 24 hours, before a third round of substrate was added and filtered out 24 hours later. A sample of the solution was taken after each round of substrate addition.

$^{238}U/^{235}U$ ratios are reported using delta notation:

$$\delta^{238}U = [(^{238}U/^{235}U)_{Sample}/(^{238}U/^{235}U)_{CRM\text{-}112A} - 1] \times 1000‰ \quad (3)$$

Equilibrium isotopic fractionation is reported in:

$$\Delta^{238}U = \delta^{238}U_{adsorbed} - \delta^{238}U_{aqueous} \quad (4)$$

$\Delta^{238}U$ was determined by fitting a linear model (see below) for each of the 8 experiments, with results from each experiment consisting of 7 data points. The initial $\delta^{238}U$ of each experiment before the addition of substrate was set at 0.01‰, the average of all U control experiments (2σ = 0.05‰). All experiments were conducted in duplicate, so two concentration and two $\delta^{238}U$ measurements were collected after each of 3 rounds of adsorption.

The experimental design involved measurement of only the aqueous U(VI) in most experiments, combined with the three rounds of adsorption, in order to produce a multiplying effect that allowed the isotopic fractionation to be determined more precisely through a mass balance model than by comparing the isotopic compositions of aqueous and adsorbed U(VI) in single-step experiments (Ellis et. al. 2004). The isotopic difference between the initial U(VI) and the final U(VI) solution following three steps of adsorption was greater than between the aqueous and adsorbed U(VI) in a single step. Therefore, this study did not choose to measure

adsorbed U(VI) for experiments 1-8 because it would have been a less precise determination of isotopic fractionation. Analytical effort that could have spent collecting redundant data for adsorbed U(VI) was instead directed toward expanding the number of experiments.

During each round of substrate addition, the $\delta^{238}U$ of the aqueous U(VI) increased as an isotopically lighter fraction was lost to adsorption. The increase in aqueous $\delta^{238}U$ is a function of $\Delta^{238}U$ and the fraction of adsorbed U(VI). With a greater fraction adsorbed, the increase seen in the aqueous U(VI) is larger, according to mass balance:

$$(\delta^{238}U_{aqueous} - \delta^{238}U_{initial}) * f_{aqueous} = -(\delta^{238}U_{adsorbed} - \delta^{238}U_{initial}) * f_{adsorbed} \quad (5)$$

where $f_{adsorbed}$ and $f_{aqueous}$ are the fractions of total U(VI) in the adsorbed and aqueous pools, respectively.

For a single step experiment, the increase in $\delta^{238}U_{aqueous}$ can be derived from equations 4 and 5:

$$\delta^{238}U_{aqueous} - \delta^{238}U_{initial} = -\Delta^{238}U * f_{adsorbed} \quad (6)$$

The cumulative effect of adsorption over three rounds is represented by the adsorption multiplier (β) which we define as a sum, over the three steps, of the fraction adsorbed in each step:

$$\beta = \Sigma^{n}_{j=1} f_{adsorbed,j} \quad (7)$$

where j is the step number and n is the total number of adsorption steps. . In the experiments, $f_{adsorbed}$ varied widely, as it was sensitive to multiple experimental parameters.

The total $\delta^{238}U$ increase in the aqueous U(VI) for the three-step process is:

$$\delta^{238}U = -\Delta^{238}U * \beta \qquad (8)$$

Accordingly, $\Delta^{238}U$ was obtained by determining the negative of the slope of a linear fit of measured $\delta^{238}U_{aqueous}$ versus β. The uncertainty of $\Delta^{238}U$ (95% confidence) is estimated as two times the standard error of the slope, which is determined using standard linear regression methods.

Although for most experiments the $\delta^{238}U$ of the adsorbed U(VI) was not determined, two experiments were conducted to ensure that the adsorbed fractions obeyed mass balance constraints. The isotopic composition of the adsorbed U(VI) was measured in two experiments (experiments 9 and 10) with the same substrate and aqueous U(VI) speciation as experiments 7 and 8 respectively. Experiments 9 and 10 aimed for a lower percentage of adsorbed U(VI) in order to create a large difference between $\delta^{238}U_{sorbed}$ and $\delta^{238}U_{initial}$. The birnessite and its adsorbed U(VI) from experiments 9 and 10 were dissolved in concentrated nitric acid over night at 80˚C. The U in the resulting solution was then analyzed. The measured $\delta^{238}U_{adsorbed}$ was compared to calculations of $\delta^{238}U_{adsorbed}$ from $\Delta^{238}U$ of experiments 7 and 8 using mass balance:

$$\delta^{238}U_{adsorbed} = (\delta^{238}U_{initial} - \delta^{238}U_{aqueous}) * (f_{aqueous}/f_{adsorbed}) + \delta^{238}U_{initial} \qquad (9)$$

U(VI) concentration and isotopic measurements

Preliminary U(VI) concentrations were measured by diluting samples 100-fold in 2% nitric acid to attain concentrations of ~5 ppb and comparing their signal intensity with a 10 ppb

standard on a Nu Plasma HR multicollector inductively coupled plasma mass spectrometer (MC-ICP-MS) at University of Illinois-Urbana Champaign. These concentration estimates were then used to spike the samples with a $^{233}U–^{236}U$ double spike that was prepared in-house with a $^{233}U/^{236}U$ of ~0.45 (Bopp et. al. 2010). The double spike method allows highly precise correction for instrumental mass bias and thus allows highly precise U isotopic analysis (Weyer et. al. 2008). An aliquot of each sample containing ~600ng U was spiked to achieve a $^{238}U/^{236}U$ ratio of ~20. The double spike then equilibrated with the sample as the mixture was evaporated to dryness and re-dissolved in 3M nitric acid. To purify the U according to Weyer et. al. (2008), the samples were passed through a column of UTEVA resin, which retains the U(VI). 3M nitric acid was added to elute interfering elements, and then U(VI) was eluted with 0.05M hydrochloric acid. The eluted U(VI) was then dried and dissolved in 2% nitric acid to attain 150ppb U.

$^{238}U/^{235}U$ of the purified U(VI) was determined on the Nu Plasma HR MC-ICPMS at University of Illinois at Urbana-Champaign. The solutions were introduced with a desolvating nebulizer (Nu Instruments DSN-100). Blank solutions of 18MΩ-cm water processed through the UTEVA resin procedure had less than 0.01ppb U, which is less than 0.01% of a typical processed sample. After tuning the instrument, several standards (IRMM REIMP-18A and CRM-129A were compared against the primary standard CRM-112A; results were determined to match previously published values before experimental solutions were measured. The samples and standards are reported in the standard delta notation, which expresses the deviation from CRM-112A in parts per thousand (per mil). The averages for 12 IRMM REIMP-18A analyses, including 6 processed through sample preparation steps alongside experimental samples, were -0.14‰±0.08‰ (2σ), while 6 CRM-129A standards averaged -1.70‰±0.06‰ (2σ). These offsets compare favorably with former studies (Weyer et. al. 2008; Shiel et. al. 2013). To measure the

drift of the MC-ICPMS, the CRM-112A standard was measured after every three samples (Bopp et. al. 2010; Weyer et. al. 2008; Brennecka et. al. 2011b). The measured $^{238}U/^{236}U$ for each sample was used to determine precisely the dissolved concentration of each sample via isotope dilution. The precision of the isotopic and concentration measurements was calculated from the results of 8 pairs of duplicate measurements, using a modified root mean square method (Hyslop and White 2009):

$$2\sigma = 2 \cdot \sqrt{\frac{\sum_{i=1}^{n}(i_a - i_b)^2}{2 \cdot n}} \qquad (10)$$

Where n is the number of duplicate pairs, i is an individual measurement, and a and b represent the two measurements of a duplicate pair.

For the 8 duplicate pairs, the calculated uncertainty was ±0.08‰ for the isotopic measurements and ±4% for concentration measurements.

CHAPTER 3- RESULTS

Time required to reach equilibrium with respect to U(VI) concentration

In the experiment designed to determine how fast the dissolved U(VI) concentration reaches equilibrium with uranyl carbonato complexes adsorbing onto goethite, concentrations stabilized within 2 hours (Table 2; Fig. 1). Although isotopic equilibrium was probably approached much more slowly, the rapid attainment of equilibrium with respect to concentration provides evidence that isotopic equilibrium is established by the end of the 24 hour equilibration period in the isotopic experiments. Additional evidence is provided below.

Results from isotopic fractionation experiments

All concentration and isotopic data, as well as $\Delta^{238}U$ calculated from eqn. 8, appear in Table 3, Fig. 2, and Fig. 3. In experiment 5b, where uranyl carbonato species were adsorbed to goethite for 65 hours, $\Delta^{238}U$ was identical, within analytical uncertainty, to that derived from the 24 hour experiment (Table 3). This strongly suggests that isotopic equilibrium was reached within 24 hours, the equilibration time in all other experiments.

Aqueous U(VI) became isotopically heavier as U(VI) was adsorbed for all experiments except experiment 2. Since adsorption made the aqueous U(VI) isotopically heavy, the adsorbed U(VI) was isotopically light. In plots of $\delta^{238}U$ vs. β, the adsorption multiplier, all data points conformed to linear models (eqn. 8) with zero intercepts, within the analytical uncertainties. The calculated isotopic fractionation between the dissolved and adsorbed U(VI), $\Delta^{238}U$, varied from 0.00‰ to -0.23‰, with 6 of 8 experiments at -0.12‰ to -0.20‰ (Table 3; Fig. 2, 3). The uncertainty of the $\Delta^{238}U$ determinations at 95% confidence (two times the standard error of the

slope of $\delta^{238}U$ vs. β) varied from 0.03‰ to 0.06‰, with lesser uncertainty for experiments with greater final β.

Results from experiments 9 and 10, in which $\delta^{238}U_{adsorbed}$ was measured for the first adsorption step, confirmed the validity of the mass balance approach used in equations 5, 8, and 9. The measured $\delta^{238}U$ values of adsorbed U(VI) for both experiments (run in duplicate) were within analytical uncertainty (±0.08‰) of the $\delta^{238}U$ values calculated using equation 9 (Table 4). Since the measured $\delta^{238}U_{adsorbed}$ for experiments 9 and 10 matched the calculated $\delta^{238}U_{adsorbed}$ from eqn. 8, our calculations are valid. This confirmation of mass balance demonstrates that there is little advantage of measuring $\delta^{238}U$ on adsorbed U(VI) aside from checking for analytical errors, which would already be obvious in the plots of $\delta^{238}U$ vs. β (Fig. 2).

The type of mineral sorbent had little or no effect on isotopic fractionation when uranyl carbonato species dominated in the aqueous phases. Calculated $\Delta^{238}U$ values all deviate from the mean value of -0.17‰ by less than their uncertainties (Fig. 3).

U(VI) speciation appeared to have a significant effect on the isotopic fractionation. The magnitude of isotopic fractionation induced by U(VI) adsorption to quartz when bicarbonate was absent was significantly less than that determined for the bicarbonate-bearing quartz experiment. The difference in $\Delta^{238}U$ between the bicarbonate-absent and bicarbonate-bearing birnessite experiments is within analytical uncertainty, but is consistent in direction with the quartz experiments. Uranyl hydroxyl ions were the dominant species in the quartz experiment at pH 6, while uranyl ions dominated the birnessite experiment at pH 3. Thus, the absence of uranyl carbonato species, or possibly other chemical variables distinguishing these two experiments from their bicarbonate-bearing counterparts, results in lesser isotopic fractionation. On the other

hand, the experiment with dominant calcium uranyl carbonato species was not significantly different from the corresponding Ca-absent experiment (Table 3; Fig. 3).

CHAPTER 4- DISCUSSION

Time to isotopic equilibrium

The goal of this study was to establish the equilibrium isotopic fractionation induced by adsorption, not temporary kinetic isotope effects initially produced by adsorption. Kinetic isotope effects may be formed initially as light isotopes diffuse and adsorb to minerals (Ellis et. al. 2004; Wasylenki et. al. 2014; Bryan et. al. 2015). However, adsorption processes usually operate over long enough time scales for isotopic equilibrium to be attained. For example, in Rifle, CO, researchers injected high concentrations of bicarbonate into the aquifer to desorb U(VI), but it still took several hours for U(VI) concentrations to increase (Fox et. al. 2012), allowing isotopic equilibrium to be approached. In most natural settings, geochemical variables affecting sorption are unlikely to change over time scales of a less than a few hours. Even if they do, subsequent stability of conditions may allow isotopic equilibrium to be attained. Thus, the results of this study should apply in most cases.

Two lines of evidence indicate that isotopic equilibrium was reached by 24 hours when most samples were taken. Because equilibrium between aqueous U(VI) concentration and the mass of U(VI) adsorbed to goethite was established in less than 2 hours, we are confident that the 24 hour equilibration time used in the isotopic experiments was sufficient to achieve isotopic equilibrium. More importantly, results from experiment 5b indicate no change in isotopic fractionation between 24 and 65 hours. We assume that these results, obtained using goethite as the sorbent, also apply to experiments using quartz, the natural aquifer material, illite, and birnessite.

Comparison to earlier studies

The isotopic fractionation we determined for equilibrium between dissolved uranyl ions and U(VI) adsorbed to birnessite compares favorably with the results of Brennecka et. al. (2011b), who found a -0.22‰ isotopic fractionation for uranyl hydroxyl species adsorbed to birnessite. Our results also agree with $\delta^{238}U$ measurements of natural ferromanganese crusts formed in the oceans. Ferromanganese crusts are isotopically light compared to seawater by an average of 0.17‰ due to adsorption of calcium uranyl carbonato complexes in the ocean (Weyer et. al 2008), similar to the $\Delta^{238}U$ (-0.13‰ to -0.23‰) induced by U(VI) adsorption to birnessite or goethite found here.

Contrastingly, desorption experiments involving bicarbonate injection at the Rifle IFRC field site suggested little to no $\delta^{238}U$ shift when U(VI) desorbed from aquifer materials (Shiel et. al. 2013). The U(VI) speciation at the Rifle IFRC site is primarily calcium uranyl carbonato complexes, which likely adsorb mostly to particles with large surface areas like clays and Fe oxides (Long et. al. 2015). Shiel et. al. (2013) reasoned that the desorption of U(VI) with $\delta^{238}U$ values ~0.2‰ less than the dissolved U(VI) should have shifted the dissolved U(VI) to lower $\delta^{238}U$ values. Based on the observation that U(VI) concentrations increased by 2x relative to the background aqueous concentration, they assumed a roughly even mixture of 0‰ background U(VI) and -0.2‰ desorbed U(VI) should lead to a -0.1‰ total U(VI) shift. Similarly, following the shut off of bicarbonate to the experiment, U(VI) re-adsorbed to aquifer minerals, resulting in a decrease in U(VI) concentrations to half the initial U(VI) concentrations. The adsorption of U(VI) was expected to produce a positive ~0.1‰ shift in the aqueous U(VI). Both the decrease and subsequent increase of 0.1‰ were not observed during the experiment (Shiel et. al. 2013).

However, in reality, the size of the observed $\delta^{238}U$ shift of the aqueous phase depends on the relative sizes of the dissolved and adsorbed U(VI) pools. For instance, if a high proportion of total U(VI) was adsorbed, the observed desorption and re-adsorption fluxes would have had little impact on the size and $\delta^{238}U$ value of adsorbed pool, which in turn control the aqueous $\delta^{238}U$. At Rifle, CO, the adsorbed U(VI) pool is thought to be approximately 5.3 times larger than the aqueous U(VI) pool under typical groundwater conditions (Fox et. al. 2012). During the desorption event when aqueous U(VI) concentrations doubled, the percent of adsorbed U(VI) would have decreased only slightly, meaning the adsorbed U(VI) pool was still dominant in terms of isotopic composition. To determine possible $\delta^{238}U$ shifts under isotopic equilibrium conditions, a mass balance model is needed to express the linkage between the dissolved and adsorbed pools:

$$\delta^{238}U_{aqueous} = \delta^{238}U_{tot} - \Delta^{238}U \times f_{adsorbed} \quad (11)$$

$$\delta^{238}U_{adsorbed} = \delta^{238}U_{tot} + \Delta^{238}U \times (1-f_{adsorbed}) \quad (12)$$

where $\delta^{238}U_{tot}$ gives the isotopic composition of the total U(VI) pool, combining adsorbed and aqueous U(VI).

The isotopic shift in aqueous U(VI) produced by adsorption/desorption can be derived as the difference between two statements of equation 11, for initial and final conditions:

$$\delta^{238}U_{aqueous,\,final} - \delta^{238}U_{aqueous,\,initial} = -\Delta^{238}U*(f_{adsorbed,\,final} - f_{adsorbed,\,initial}) \quad (13)$$

Given that initially the adsorbed U(VI) pool was approximately 5.3 times larger than the aqueous U(VI) pool, the $f_{adsorbed,\ initial}$=0.84. The desorption due to bicarbonate would produce a $f_{adsorbed,final}$= 0.68, producing, for $\Delta^{238}U$= -0.20‰, a total isotopic shift in aqueous U(VI) of -0.03‰. The decrease in concentration due to re-adsorption would produce a $f_{adsorbed,final}$ value of 0.92, producing an isotopic shift in aqueous U(VI) of 0.02‰. Thus, the total expected shift through the entire desorption/adsorption cycle would be only 0.05‰, less than the uncertainty of the isotopic measurements. In essence, because the adsorbed pool was very large, it was changed little by the desorption and re-adsorption processes, and acted as a $\delta^{238}U$ buffer.

Mechanism of isotopic fractionation

Brennecka et. al. (2011b) found significant differences between EXAFS spectra obtained for aqueous and adsorbed U(VI); this supported their hypothesis that shifts in coordination geometry drive isotopic fractionation. While Brennecka et. al. (2011b) could not determine precisely the difference in coordination of the U atom caused by inner sphere adsorption, a more recent study did find loss of symmetry for uranyl ions adsorbed to birnessite (Rihs et. al. 2014). Similar loss of symmetry has been seen for U(VI) adsorption to goethite, quartz, and clays (Singh et. al. 2012; Greathouse et. al. 2002; Catalano and Brown 2005). Since loss of symmetry of equatorial oxygens around U is seen for all minerals, it is not surprising that isotopic fractionation occurs for all the solid phases studied. The data from the present study and the EXAFS data conform to a consistent model of bonding changes accompanying adsorption.

The bicarbonate-absent experiment with quartz and the sorbent is the lone exception to this model. Given the previous studies' results from EXAFS, it is expected that the adsorbed U(VI) in the quartz experiment should have a coordination similar to that in the other

experiments. However, this experiment was unusual in that it contained few ions in solution aside from U(VI) and relatively few inner sphere bonding sites available. Under these conditions, we speculated that only a small fraction of the U(VI) occupied all inner sphere adsorption sites, leaving U(VI) ions primarily adsorbed as outer sphere complexes. The lack of isotopic fractionation suggests such a mechanism, as it would allow the adsorbed U(VI) coordination to be closely similar to that in the aqueous phase.

Applications of U(VI) isotopic fractionation induced by adsorption

The occurrence of isotopic fractionation due to adsorption affects the interpretation of $\delta^{238}U$ variations related to U(VI) reduction in contaminated aquifers. Given rates of equilibration observed here, adsorbed and aqueous U(VI) should remain in isotopic equilibrium. With groundwater chemistry changing as bicarbonate or calcium concentrations change, the proportion of adsorbed and dissolved U(VI) will change, producing isotopic shifts. One U remediation strategy involves the injection of bicarbonate to desorb U(VI), followed by injection of acetate to reduce it. Applying isotopic methods to estimate % reduction could lead to overestimation of amount reduced. Desorption of an isotopically light U(VI) pool will produce a negative isotopic shift in the aqueous U(VI); this negative shift will augment the negative shift occurring during U reduction, leading to an overestimation of the extent of reduction. In the case of the previous Rifle IFRC desorption experiments described above, desorption is expected to produce a shift of only 0.03‰, relative to the ~1‰ shift caused by reduction. In cases of stronger desorption, greater effects would occur, so the effect should be considered in context of the individual study. Overall, studies using $\delta^{238}U$ data to assess U(VI) reduction must consider adsorption as a lesser, but significant fractionating process.

To correctly interpret ancient marine $\delta^{238}U$ data, researchers must understand the isotopic fractionations accompanying all removal mechanisms. U(VI) in the oceans is removed primarily through reduction of U(VI) to U(IV) in organic-rich sediments, incorporation into biogenic carbonate, and sequestration in oceanic crust during weathering (Dunk et. al. 2002). Adsorption of U(VI) by ferromanganese oxides is a minor removal mechanism of oceanic U(VI) in the modern oceans (Klinkhammer and Palmer 1991; Dunk et. al. 2002), and thus the process does not greatly affect oceanic $\delta^{238}U$ values. However, there may be some times and locations in earth history where adsorption was a more important process (e.g., during deposition of banded iron formations). Since we know the fractionation accompanying adsorption to a range of oxide and silicate materials, we have a better idea of the isotopic composition of the burial flux of adsorbed U(VI). This knowledge should help paleoredox studies.

Future Work

This study has determined variations in $\Delta^{238}U$ for equilibrium adsorption over a range of conditions. Although these experiments strived to test the most environmentally relevant mineral sorbents and U(VI) speciation conditions, several more chemical conditions may be measured to provide an even broader picture of adsorption effects on U(VI) measurements. U(VI) adsorption to calcite can be common in karst aquifers, so investigating the isotopic behavior of adsorbed U(VI) to calcite may prove helpful in better understanding these systems. In addition, coprecipitation of U(VI) with carbonate minerals is one of the major removal mechanisms of U(VI) in the oceans (Dunk et. al. 2002). The adsorption of U(VI) to calcite might be expected to produce a ~ -0.2‰ isotopic fractionation, similar to the minerals in this study, but recent research suggests little to no isotopic fractionation is produced. In the Bahamas, carbonates and seawater,

which were almost certainly in isotopic equilibrium, had identical isotope ratios (Romaniello et. al. 2013). A laboratory experiment found that coprecipitation of U(VI) with calcite produced no resolvable isotopic fractionation, but this experiment did not demonstrably achieve isotopic equilibrium (Chen et. al. 2014). A controlled experiment measuring the equilibrium isotopic fractionation between aqueous U(VI) and U(VI) adsorbed to calcite would be valuable in providing additional evidence of a lack of isotopic fractionation due to U(VI) removal by carbonates. In addition, U(VI) phosphate ($UO_2PO_4^-$ and $UO_2HPO_{4(aq)}$) complexes can occur under certain conditions in groundwater and surface water; future work on U isotopic fractionation induced by adsorption of these complexes might be useful.

CHAPTER 5- CONCLUSIONS

The adsorption of U(VI) to goethite, birnessite, illite, aquifer material, and quartz produced an average isotopic fractionation of -0.17‰ with adsorbed U(VI) isotopically lighter than aqueous U(VI). The minerals tested in this study all produced similar isotopic fractionations with uranyl carbonato species adsorbed to quartz, illite, aquifer material, goethite, and birnessite producing fractionations that were within uncertainty of each other. Aqueous speciation had a larger effect with uranyl carbonato and calcium uranyl carbonato complexes producing a greater isotopic fractionation than uranyl hydroxyl species. Uranyl hydroxyl ions adsorbing to quartz did not produce any isotopic fractionation.

U isotope ratios are increasingly being used as indicators of U redox reactions, and the effects of adsorption processes on $^{238}U/^{235}U$ data must be accounted for. Based on the present study, $\delta^{238}U$ of U(VI) adsorbed to silicate and oxide solids can be assumed to be about -0.17‰ less than coexisting water under most conditions. Our results suggest that adsorption cannot cause fractionations as large as reduction, but generally causes significant fractionation that have a second order effect. This study represents the first direct measurement of isotopic fractionation induced by adsorption of U(VI) species relevant to seawater. Paleoredox studies of the ancient ocean could be affected by U(VI) adsorption to ferromanganese oxides if the amount of ferromanganese oxides produced was very large at certain times.

CHAPTER 6- FIGURES AND TABLES

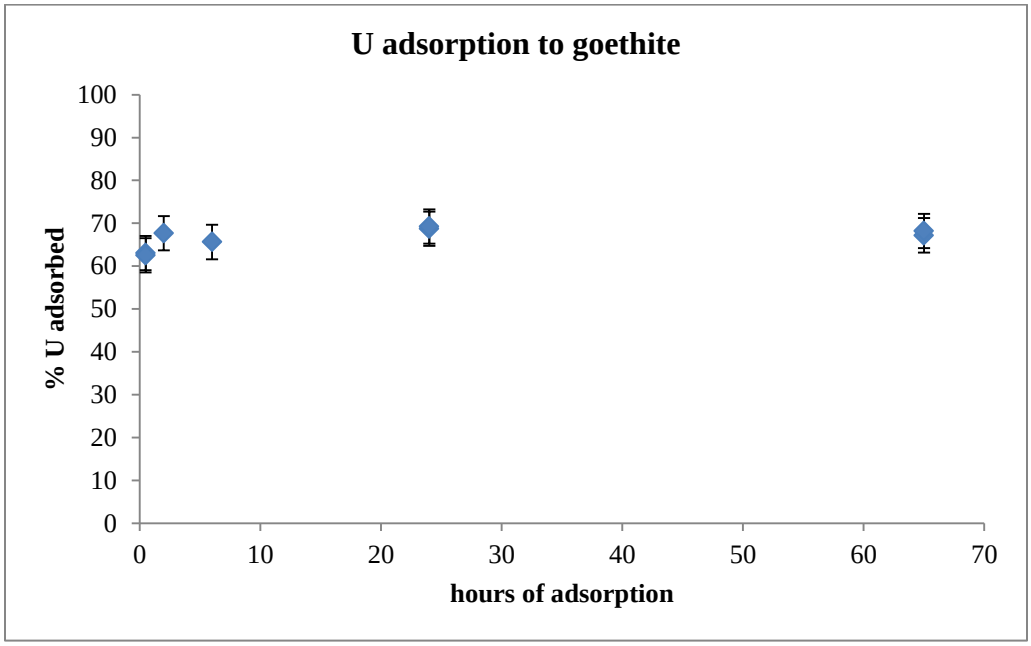

Fig. 1: U adsorption to goethite over time. It appears chemical equilibrium was reached within 2 hours.

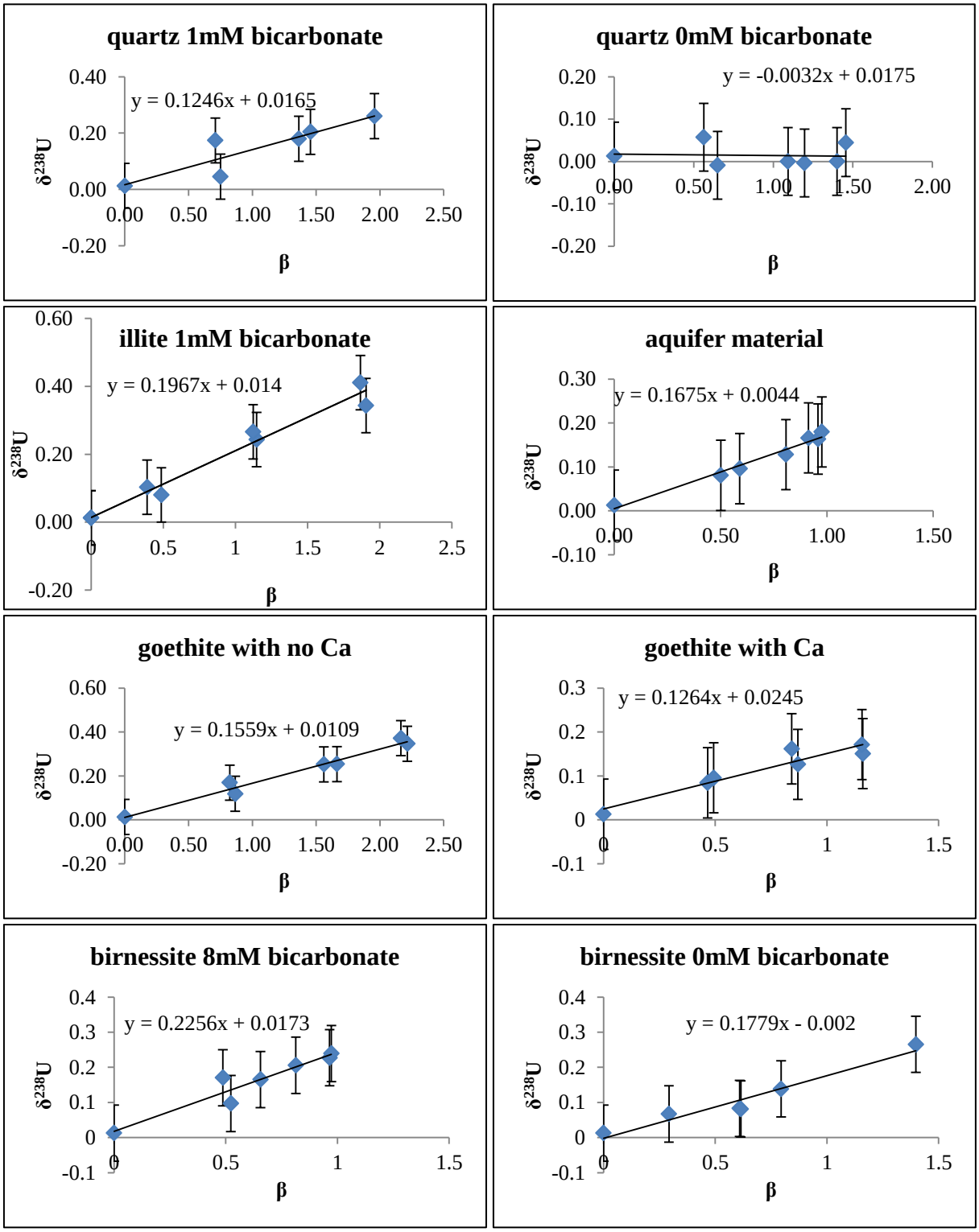

Fig. 2: $\delta^{238}U_{aqueous}$ versus β for all experiments. $\Delta^{238}U$ is determined as the negative of the slope.

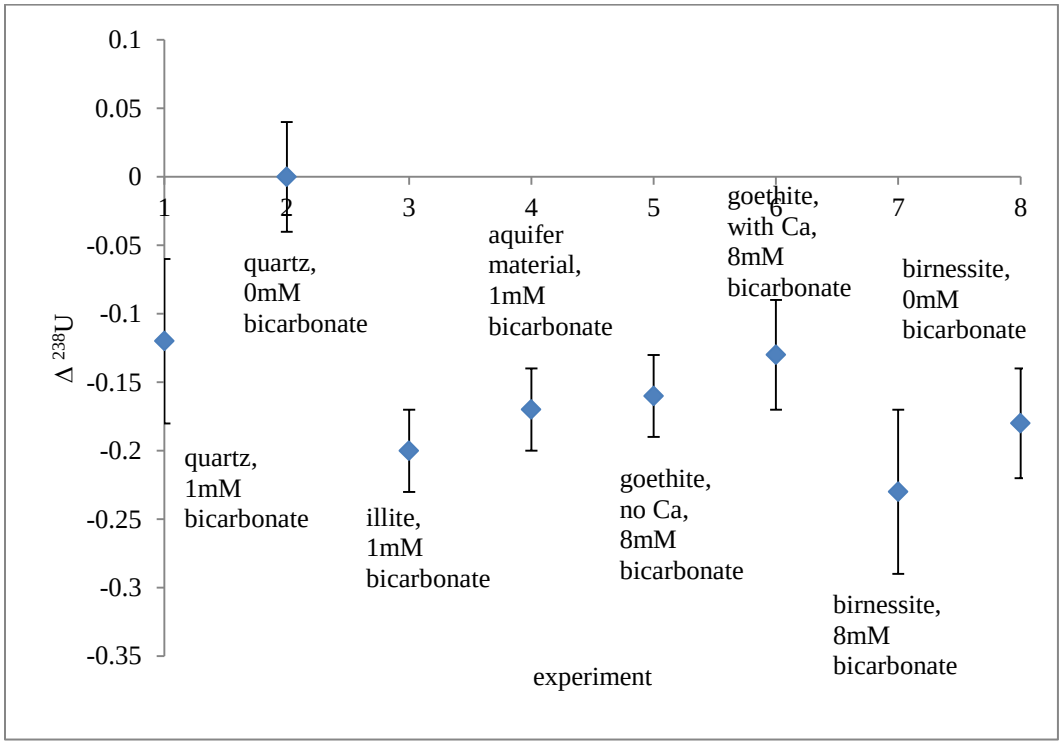

Fig. 3: Isotopic fractionation between aqueous U(VI) and adsorbed U(VI) for all experiments

Table 1: List of experiments performed

Experiment	Substrate	Mass (g)	[HCO3] (mM)	pH	Major U(VI) species*
1	quartz	15	1	8	$UO_2(CO_3)_2^{2-}$, $UO_2(CO_3)_{(aq)}$
2	quartz	1	0	6	$UO_2(OH)^+$, $(UO_2)_3(OH)_5^+$
3	illite	0.4	1	8	$UO_2(CO_3)_2^{2-}$, $UO_2(CO_3)_{(aq)}$
4	aquifer material	0.2	1	8	$UO_2(CO_3)_2^{2-}$, $UO_2(CO_3)_{(aq)}$
5	goethite	0.085	8	8	$UO_2(CO_3)_2^{2-}$, $UO_2(CO_3)_3^{4-}$
6	goethite	0.32	8	8	$Ca_2UO_2(CO_3)_{3(aq)}$, $CaUO_2(CO_3)_3^{2-}$
7	birnessite	0.037	8	8	$UO_2(CO_3)_2^{2-}$, $UO_2(CO_3)_3^{4-}$
8	birnessite	0.0037	0	3	UO_2^{2+}

*Calculated by Visual MINTEQ (Gustafsson 2011).

Table 2: Adsorption to goethite over time

Sample (duration)	Concentration	% adsorbed
U control	1046	0
30min #1	354	63
30min #2	359	63
2hr	309	68
6hr	329	66
24hr #1	299	69
24hr #2	294	69
65hr #1	314	67
65hr #2	304	68

Table 3: Concentration and isotopic data for all experiments

	Concentration (ppb) (bottle 1)	Concentration (ppb) (bottle 2)	$\delta^{238}U$ (‰) (bottle 1)	$\delta^{238}U$ (‰) (bottle 2)
Expt. #1				
Quartz 1mM DIC pH 8				
control	1072		0.00	
1st step	311	268	0.17	0.05
2nd step	100	73	0.18	0.20
3rd step	38		0.26	
calculated Δ^{238U} (in ‰)			-0.12	±0.06
Expt. #2				
Quartz 0mM DIC pH 6				
control	1017		0.00	
1st step	445	356	0.06	-0.01
2nd step	153	186	0.00	0.00
3rd step	106	121	0.04	0.00
calculated Δ^{238U} (in ‰)			0.00	±0.04
Expt. #3				
Illite 1mM DIC pH 8				
control	1302		0.06	
1st step	680	782	0.08	0.10
2nd step	231	208	0.24	0.27
3rd step	56	53	0.41	0.34
calculated Δ^{238U} (in ‰)			-0.20	±0.03
Expt. #4				
Aquifer material 1mM DIC pH 8				
control	1072		0.00	
1st step	535	440	0.08	0.10
2nd step	348	279	0.13	0.17
3rd step	277	245	0.16	0.18
calculated Δ^{238U} (in ‰)			-0.17	±0.03
Expt. #5a				
Goethite 8mM DIC pH 8				
control	1078		0.01	
1st step	145	191	0.12	0.17
2nd step	27	47	0.25	0.25
3rd step	12	17	0.35	0.37
calculated Δ^{238U} (in ‰)			-0.16	±0.03

Table 3 continued

	Concentration (ppb) (bottle 1)	Concentration (ppb) (bottle 2)	$\delta^{238}U$ (‰) (bottle 1)	$\delta^{238}U$ (‰) (bottle 2)
Expt. #5b Goethite 8mM DIC pH 8 equilibrated for 65 hours				
control	1078	0.01		
1st step	122	170	0.16	0.15
calculated Δ^{238U} (in ‰)			-0.17	±0.03
Expt. #6 Goethite 8mM DIC pH 8 with Ca				
control	1122		0.00	
1st step	599	569	0.08	0.10
2nd step	335	347	0.13	0.16
3rd step	223	223	0.15	0.17
calculated Δ^{238U} (in ‰)			-0.13	±0.04
Expt. #7 Birnessite 8mM DIC pH 8				
control	1133		0.00	
1st step	581	540	0.17	0.10
2nd step	453	359	0.17	0.21
3rd step	293	283	0.23	0.24
calculated Δ^{238U} (in ‰)			-0.23	±0.06
Expt. #8 Birnessite 0mM DIC pH 3				
control	1085		0.04	
1st step	734	440	0.07	0.08
2nd step	502	95	0.08	0.27
3rd step	409		0.14	
calculated Δ^{238U} (in ‰)			-0.18	±0.04

Table 4: Measured and calculated $\delta^{238}U$ of adsorbed U(VI) in experiments 9 and 10

Experiment	**% adsorbed**	**$\delta^{238}U_{calculated}$**	**$\delta^{238}U_{measured}$**
9 bottle 1	7	-0.20	-0.13
9 bottle 2	5	-0.21	-0.19
10 bottle 1	19	-0.13	-0.12
10 bottle 2	25	-0.12	-0.14

CHAPTER 7- REFERENCES

Abdelouas, A. Uranium mill tailings: geochemistry, mineralogy, and environmental impact. *Elements* **2006**, 2, 335-341.

Abe, M; Suzuki, T; Fujii, Y; Hada, M; Hirao, K. An ab initio molecular orbital study of the nuclear volume effects in uranium isotope fractionations. *J. Chem. Phys.* **2008**, 129, 164309.

Anderson, RT; Vrionis, HA; Ortiz-Bernad, I; Resch, CT; et. al. Stimulating the in situ activity of Geobacter species to remove uranium from the groundwater of a uranium-contaminated aquifer. *Appl. Environ. Microbiol.* **2003**, 69, 5884-5891.

Asael, D; Tissot, FLH; Reinhard, CT; Rouxel, O; et. al. Coupled molybdenum, iron and uranium stable isotopes as oceanic paleoredox proxies during the Paleoproterozoic Shunga Event. *Chem. Geol.* **2013**, 362, 193-210.

Bargar, JR; Reitmeyer, R; Lenhart, JJ; Davis, JA. Characterization of U (VI)-carbonato ternary complexes on hematite: EXAFS and electrophoretic mobility measurements. *Geochim. Cosmochim. Acta* **2000**, 64, 2737-2749.

Basu, A; Sanford, RA; Johnson, TM. Uranium isotopic fractionation factors during U (VI) reduction by bacterial isolates. *Geochim. Cosmochim. Acta* **2014**, 136, 100-113.

Bigeleisen, J. Nuclear Size and Shape Effects in Chemical Reactions. Isotope Chemistry of the Heavy Elements. *JACS* **1996**, 118, 3676-3680.

Bopp, CJ; Lundstrom, CC; Johnson, TM. Uranium 238U/235U isotope ratios as indicators of reduction: results from an in situ biostimulation experiment at Rifle, Colorado, USA. *Environ. Sci. Technol.* **2010**, 44, 5927-5933.

Bopp, CJ; Lundstrom, CC; Johnson, TM; Glessner, JJG. Variations in 238U/235U in uranium ore deposits: isotopic signatures of the U reduction process?. *Geology* **2009**, 37, 611-614.

Brennecka, GA; Borg, LE; Hutcheon, ID; Sharp, MA. Natural variations in uranium isotope ratios of uranium ore concentrates: Understanding the 238 U/235 U fractionation mechanism. *Earth Planet. Sci. Lett.* **2010**, 291, 228-233.

Brennecka, GA; Herrmann, AD; Algeo, TJ; Anbar, AD. Rapid expansion of oceanic anoxia immediately before the end-Permian mass extinction. *PNAS* **2011a**, 108, 17631-17634.

Brennecka, GA; Wasylenki, LE; Bargar, JR; Weyer, S; Anbar, AD. Uranium Isotope Fractionation during Adsorption to Mn-Oxyhydroxides. *Environ. Sci. Technol.* **2011b**, 45, 1370-1375.

Bryan, AL; Dong, S; Wilkes, EB; Wasylenki, LE. Zinc isotope fractionation during adsorption onto Mn oxyhydroxide at low and high ionic strength. *Geochim. Cosmochim. Acta* **2015**, 157, 182-197.

Campbell, KM; Kukkadapu, RK; Qafoku, NP. Geochemical, mineralogical and microbiological characteristics of sediment from a naturally reduced zone in a uranium-contaminated aquifer. *Appl. Geochem.* **2012**, 27, 1499-1511.

Catalano, JG; Brown, GE, Jr. Uranyl adsorption on montmorillonite: evaluation of binding sites and carbonate complexation. *Geochim. Cosmochim. Acta* **2005**, 69, 2995-3005.

Chen, X; Romaniello, S; Herrmann, A; Wasylenki, L; Anbar, A. Uranium Isotope Fractionation During Coprecipitation with Aragonite and Calcite. *AGU Fall Meeting* **2014**, PP51C-1141.

Dahl, TW; Boyle, RA; Canfield, DE; Conelly, JN; et. al. Uranium isotopes distinguish two geochemically distinct stages during the later Cambrian SPICE event. *Earth Planet. Sci. Lett.* **2014**, 401, 313-326.

Dunk, RM; Mills, RA; Jenkins, WJ. A reevaluation of the oceanic uranium budget for the Holocene. *Chem. Geol.* **2002**, 190, 45-67.

Ellis, AS; Johnson, TM; Bullen, TD. Using chromium stable isotope ratios to quantify Cr (VI) reduction: lack of sorption effects. *Environ. Sci. Technol.* **2004**, 38, 3604-3607.

Fox, PM; Davis, JA; Hay, MB; Conrad, ME; et. al. Rate-limited U(VI) desorption during a small-scale tracer test in a heterogeneous uranium-contaminated aquifer. *Water Resour. Res.* **2012**, 48, W05512.

Fox, PM; Davis, JA; Zachara, JM. The effect of calcium on aqueous uranium(VI) speciation and adsorption to ferrihydrite and quartz. *Geochim. Cosmochim. Acta* **2006**, 70, 1379-1387.

Fujii, Y; Higuchi, N; Haruno, Y; Nomura, M. Temperature dependence of isotope effects in uranium chemical exchange reactions. *J. Nucl. Sci. Technol.* **2006**, 43, 400-406.

Goto, KT; Anbar, AD; Gordon, GW; Romaniello, SJ; et. al. Uranium isotope systematics of ferromanganese crusts in the Pacific Ocean: Implications for the marine 238U/235U isotope system. *Geochim. Cosmochim. Acta* **2014**, 146, 43-58.

Greathouse, JA; O'Brien, RJ; Bemis, G; Pabalan, RT. Molecular Dynamics Study of Aqueous Uranyl Interactions with Quartz (010). *J. Phys. Chem. B* **2002**, 106, 1646-1655.

Grimm, TR; Johnson, TM. Isotopic Study of Uranium: Determining the Isotopic Fractionation of Uranium During Abiotic Reduction with Iron(II). *University of Illinois Master's Thesis* **2014**.

Gustafsson, JP. Visual MINTEQ ver. 3.0. *KTH* **2011**.

Hobday, DK; Galloway, WE. Groundwater processes and sedimentary uranium deposits. *Hydrol. J.* **1999**, 7, 127-138.

Hsi, CD; Langmuir, D. Adsorption of uranyl onto ferric oxyhydroxides: application of the surface complexation site-binding model. *Geochim. Cosmochim. Acta* **1985**, 49, 1931-1941.

Hyslop, NP; White, WH. Estimating Precision Using Duplicate Measurements. *J. Air Waste Manag. Assoc.* **2009**, 59, 1032-1039.

Ilton, ES; Wang, Z; Boily, J-F; Qafoku, O; Rosso, KM; Smith, SC. The effect of pH and time on the extractability and speciation of uranium(VI) sorbed to SiO2. *Environ. Sci. Technol.* **2012**, 46, 6604-6611.

Kendall, B; Brennecka, GA; Weyer, S; Anbar, AD. Uranium isotope fractionation suggests oxidative uranium mobilization at 2.50 Ga. *Chem. Geol.* **2013**, 362, 105-114.

Kendall, B; Komiya, T; Lyons, TW; Bates, SM; et. al. Uranium and molybdenum isotope evidence for an episode of widespread ocean oxygenation during the late Ediacaran Period. *Geochim. Cosmochim. Acta* **2015**, 156, 173-193.

Klinkhammer, GP; Palmer, MR. Uranium in the oceans: Where it goes and why. *Geochim. Cosmochim. Acta* **1991**, 55, 1799-1806.

Long, PE; Williams, KH; Davis, JA; Fox, PM. Bicarbonate impact on U (VI) bioreduction in a shallow alluvial aquifer. *Geochim. Cosmochim. Acta* **2015**, 150, 106-124.

Montoya-Pino, C; Weyer, S; Anbar, AD; Pross, J. Global enhancement of ocean anoxia during Oceanic Anoxic Event 2: A quantitative approach using U isotopes. *Geology* **2010**, 38, 315-318.

Murphy, MJ; Stirling, CH; Kaltenbach, A; Turner, SP; Schaefer, BF. Fractionation of 238U/235U by reduction during low temperature uranium mineralisation processes. *Earth Planet. Sci. Lett.* **2014**, 388, 306-317.

Rieder, M; Cavazzini, G; D'Yakanov, YS; Frank-Kamenetskii, VA; et. al. Nomenclature of the Micas. *Can. Mineral.* **1998**, 36, 905-912.

Rihs, S; Gaillard, C; Reich, T; Kohler, SJ. Uranyl sorption onto birnessite: A surface complexation modeling and EXAFS study. *Chem. Geol.* **2014**, 373, 59-70.

Romaniello, SJ; Herrmann, AD; Anbar, AD. Uranium concentrations and 238U/235U isotope ratios in modern carbonates from the Bahamas: Assessing a novel paleoredox proxy. *Chem. Geol.* **2013**, 362, 305-316.

Schauble, EA. Equilibrium uranium isotope fractionation by nuclear volume and mass-dependent processes. *AGU Fall Meeting* **2006**, V21B-0570.

Shiel, AE; Laubach, PG; Johnson, TM; Lundstrom, CC; Long, PE; Williams, KH. No Measurable Changes in 238U/235U due to Desorption−Adsorption of U(VI) from Groundwater at the Rifle, Colorado, Integrated Field Research Challenge Site. *Environ. Sci. Technol.* **2013**, 47, 2535-2541.

Singh, S; Catalano, JG; Ulrich, K-U; Giammar, DE Molecular-scale structure of uranium(VI) immobilized with goethite and phosphate. *Environ. Sci. Technol.* **2012**, 46, 6594-6603.

Stewart, BD; Mayes MA; Fendorf S. Impact of uranyl-calcium carbonato complexes on U(VI) adsorption to synthetic and natural sediments. *Environ. Sci. Technol.* **2010**, 44, 928-934.

Stirling, CH; Andersen, MB; Potter, EK. Low-temperature isotopic fractionation of uranium. *Earth Planet. Sci. Lett.* **2007**, 264, 208-225.

Stroes-Gascoyne, S; Kramer, JR; Snodgrass, WJ. Preparation, characterization and aging of δ-MnO2, for use in trace metal speciation studies. *Appl. Geochem.* **1987**, 2, 217-226.

Stylo, M; Neubert, N; Wang, Y; Monga, N; Romaniello, SJ; Weyer, S; Bernier-Latmani, R. Uranium isotopes fingerprint biotic reduction. *PNAS* **2015**, 112, 5619-5624.

Sylwester, ER; Hudson, EA; Allen, PG. The structure of uranium (VI) sorption complexes on silica, alumina, and montmorillonite. *Geochim. Cosmochim. Acta* **2000**, 64, 2431-2438.

Tribovillard, N; Algeo, TJ; Lyons, T; Riboulleau, A. Trace metals as paleoredox and paleoproductivity proxies: An update. *Chem. Geol.* **2006**, 232, 12-32.

Uranium Mill Tailings Radiation Control Act (UMTRCA) Sites Fact Sheet. *US Department of Energy* **2013**.

Waite, TD; Davis, JA; Payne, TE; Waychunas, GA; Xu, N. Uranium (VI) adsorption to ferrihydrite: Application of a surface complexation model. *Geochim. Cosmochim. Acta* **1994**, 58, 345-359.

Wall, JD; Krumholz, LR. Uranium reduction. *Annu. Rev. Microbiol.* **2006**, 60, 149-166.

Wang, X; Johnson, TM; Lundstrom, CC. Low temperature equilibrium isotope fractionation and isotope exchange kinetics between U(IV) and U(VI). *Geochim. Cosmochim. Acta* **2015**, 158, 262-275.

Wasylenki, LE; Rolfe, BA; Weeks, CL; Spiro, TG; Anbar, AD. Experimental investigation of the effects of temperature and ionic strength on Mo isotope fractionation during adsorption to manganese oxides. *Geochim. Cosmochim. Acta* **2008**, 72, 5997-6005.

Wasylenki, LE; Swihart, JW; Romaniello, SJ. Cadmium isotope fractionation during adsorption to Mn oxyhydroxide at low and high ionic strength. *Geochim. Cosmochim. Acta* **2014**, 140, 212-226.

Weyer, S; Anbar, AD; Gerdes, A; Gordon, GW; Algeo, TJ; Boyle, EA. Natural fractionation of 238U/235U. *Geochim. Cosmochim. Acta* **2008**, 72, 345-359.

Ylagan, RF; Altaner, SP; Pozzuoli, A. Reaction mechanisms of smectite illitization associated with hydrothermal alteration from Ponza Island, Italy. *Clays Clay Mineral.* **2000**, 48, 610-631.